Desalination 520 (2021) 115316

Contents lists available at ScienceDirect

Desalination

journal homepage: www.elsevier.com/locate/desal

Reclaiming wastewater with increasing salinity for potable water reuse: Water recovery and energy consumption during reverse osmosis desalination

Xin Wei [*], Kelly T. Sanders, Amy E. Childress

Sonny Astani Department of Civil and Environmental Engineering, University of Southern California, Los Angeles, CA 90089, United States

HIGHLIGHTS

- Wastewater salinity is increasing and climate change exacerbates it.
- Desalination of higher-salinity streams along with wastewater has multiple benefits.
- Rate of energy increase decreases with increasing salinity.
- ERD and CCRO enable removal of additional salinity at no additional energy cost.

GRAPHICAL ABSTRACT

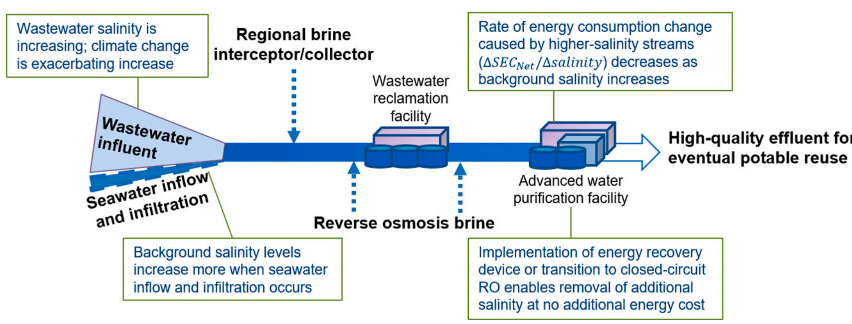

ARTICLE INFO

Keywords:
Reverse osmosis desalination
Potable water reuse
Energy consumption
Higher salinity streams
Energy saving strategies

ABSTRACT

With reverse osmosis membranes being industry-standard in many potable reuse facilities, an opportunity exists to desalinate higher-salinity streams (e.g., brine and regional brine interceptor streams) to augment traditional wastewater supplies and reduce brine disposal requirements. This study evaluates the energy consumed in recovering water from these streams at advanced water purification facilities. Scenarios without and with seawater inflow and infiltration at coastal wastewater reclamation facilities are considered. It was found that as wastewater salinity increases with increasing seawater inflow and infiltration, base case energy consumption increases, but the percent increase of energy consumption caused by mixing higher-salinity streams decreases. Multiple energy-saving strategies were evaluated, including energy recovery devices, closed-circuit reverse osmosis, and desalination of the higher-salinity streams separately from the treated wastewater. The energy savings was greater for closed-circuit reverse osmosis than for energy recovery devices and increased for both as influent salinity increases. The energy savings from desalinating higher-salinity streams separately increased as the salinity difference between the two streams increased. Addition of higher-salinity streams was also considered within the context of inorganic scaling potential, product water requirements, and discharge permits that may limit recoveries.

* Corresponding author.
E-mail address: wei383@usc.edu (X. Wei).

https://doi.org/10.1016/j.desal.2021.115316
Received 26 June 2021; Received in revised form 18 August 2021; Accepted 24 August 2021
Available online 8 September 2021
0011-9164/

1. Introduction

1.1. Trends in potable reuse

Potable reuse, or the process of converting wastewater into water that can be reused for potable purposes, is a well-established practice to provide a local, drought-proof water supply in water-scarce regions [1,2]. Conversion of wastewater to potable water may begin at a wastewater treatment or reclamation facility and continue at an advanced water purification facility (AWPF); alternatively, a wastewater reclamation facility may be retrofitted with advanced water treatment processes if space is available.

The US is a leader in potable reuse projects [3]. Orange County Water District's (OCWD's) Groundwater Replenishment System, which is currently undergoing expansion from 3.8×10^5 to 4.9×10^5 m^3/day (100 to 130 million gallons/day (MGD)) production capacity, is the world's largest AWPF for indirect potable reuse via groundwater recharge. According to the 2017 Potable Reuse Compendium [4], potable reuse installations are expected to increase in the US and internationally. For example, Singapore operates five NEWater facilities that reclaim wastewater mostly for high-quality industrial use but also for indirect potable reuse via reservoir augmentation. The NEWater facilities are expected to meet up to 55% of Singapore's water demand by 2060 [5].

As the volume of wastewater being reclaimed for potable reuse has significantly increased in the past 10–20 years, reverse osmosis (RO) installations have proliferated [6–11]. In California, potable reuse regulations require AWPFs to have RO processes when the product water is being directly injected into the groundwater or being used for reservoir augmentation [12]. The RO process separates contaminants such as pathogens, disinfection byproducts, and trace organic compounds [13–16] as well as dissolved solids/salinity.

1.2. Role of desalination in potable reuse

Over the last decades, salinity levels in wastewater have increased, in large part due to residential water treatment systems (e.g., water softeners and septic systems) [17], industrial uses [18], water conservation measures [19], operation of desalination systems at upstream facilities, and also, in coastal regions, seawater inflow and infiltration (I&I) [20]. At coastal wastewater reclamation facilities located at low elevation, leaky gates, corroded pipes, and aging infrastructure may allow seawater to pass through sewage conveyance pipes and connections and intrude into wastewater reclamation facilities [21]. Hence, while the role of RO membranes in separating pathogens and trace organic compounds is still key, the role of RO membranes in separating salts for potable reuse applications is being rediscovered as critical.

With RO membranes being industry-standard at most AWPFs [22,23], an opportunity exists to desalinate higher-salinity streams (e.g., brine and regional brine interceptor streams), to augment traditional wastewater supplies. If higher-salinity streams are discharged to a wastewater reclamation facility that supplies an AWPF, the salinity from these streams is conserved through the wastewater treatment processes and would then be separated by the RO process at the AWPF. Desalination of the higher-salinity stream along with treated wastewater would increase the supply of water available for potable reuse while at the same time, reduce the volume of discharge, which may be useful depending on the ultimate discharge goal. Recovering water from the higher-salinity stream imparts value to this impaired water source that is otherwise considered a waste stream. Also, dilution with the treated wastewater may reduce the inorganic scaling potential associated with these streams.

1.3. Higher-salinity streams

In this paper, "higher-salinity streams" refers to brackish water RO (BWRO) brine and regional brine interceptor/collector streams that have salinities greater than 2 g/L (i.e., greater than the salinity of typical wastewater) [24,25]. BWRO facilities for inland groundwater desalination typically produce brines with salinities greater than 10 g/L and TOC concentrations less than 15 mg/L [26–29]. The cost to dispose the brines ranges from 5 to 33% of the total cost of desalination [30]. Also, brine discharge regulations often limit the capacity of BWRO facilities [31]. Some BWRO facilities discharge their brine to a regional brine interceptor that conveys the brine to a wastewater reclamation facility, where it is treated prior to ocean discharge [32]. A well-known example of a regional brine interceptor is the Inland Empire Brine Line in Southern California, USA. The Inland Empire Brine Line conveys combined flows of brines from desalters, concentrated waste streams, and effluent from the treatment facility of a hazardous waste site. With a capacity of 30 MGD, the Inland Empire Brine Line has an average flowrate of 12 MGD, an average salinity (in 2020) of 5.7 g/L [33], and a TOC concentration of approximately 7 mg/L [32,33]. The Inland Empire Brine Line becomes the Santa Ana Regional Interceptor, which includes local wastewater collected along the pipeline alignment in Orange County. Due to higher salinity levels and irregular discharges that may occur in the Inland Empire Brine Line, the Santa Ana Regional Interceptor flow is treated as a separate flow by the Orange County Sanitation District. Unlike wastewater in the trunk sewer line, the treated Santa Ana Regional Interceptor flow is discharged to the ocean and is not used as source water for potable reuse through the Groundwater Replenishment System [34].

1.4. Energy recovery devices and closed-circuit RO

Two-stage RO, where the concentrate from the first stage becomes the feed to the second stage (Fig. 1a), is often used in AWPF RO and BWRO processes to increase water recovery [35]. Two-stage RO reduces the specific energy consumption (*SEC*) of the desalination process by decreasing the irreversible work (i.e., the energy lost) in the desalination process [36].

High energy costs in the water sector have led many water and wastewater treatment facilities to include energy management strategies as part of their daily operation [37,38]. For example, energy recovery devices (ERDs) are commonly used in conjunction with high-salinity RO processes (e.g., seawater RO) to provide specific energy savings (*SES*) and reduce the *SEC* of the desalination process [39–41]. ERDs reduce energy consumption by transferring the energy left in the RO concentrate back to the feed stream via centrifugal or positive displacement isobaric devices (e.g., pressure exchangers and turbochargers) [42]. ERDs can reduce the energy consumption at seawater RO desalination facilities by as much as 67%, depending on operating conditions. In BWRO facilities and AWPFs, although ERDs can be used (Fig. 1b) the low influent salinity and relatively low brine flowrate make the benefits of ERDs ambiguous [43]. Although ERDs are not commonly used in AWPFs (see Table S.2), if higher-salinity streams are considered for augmenting influent, use of an ERD may become beneficial.

High-recovery RO processes (e.g., closed-circuit reverse osmosis (CCRO)) are being considered at AWPFs to improve water recovery while keeping energy consumption low [44]. CCRO is a semi-batch process in which the brine is recirculated while water permeates through the RO membrane (Fig. 1c). Pressurized influent is continuously added to the brine, which is not depressurized, and the mixture is returned to the membrane module to be separated. Once a desired water recovery is reached, the brine stream is ejected and replaced by new feed solution [44]. For lower-salinity and lower-brine-flowrate applications, such as in AWPF RO and BWRO processes, CCRO can provide *SES* because the irreversible energy consumed in RO is decreased by operating with time-variant feed pressure [44]. In this way, CCRO may provide greater water and energy benefits than ERDs [44]. Model results from Warsinger et al. [44]. predict that CCRO can have up to 37% less energy requirements than a standard BWRO process operating at high (90%) water-recovery. Other than achieving high water-recovery with

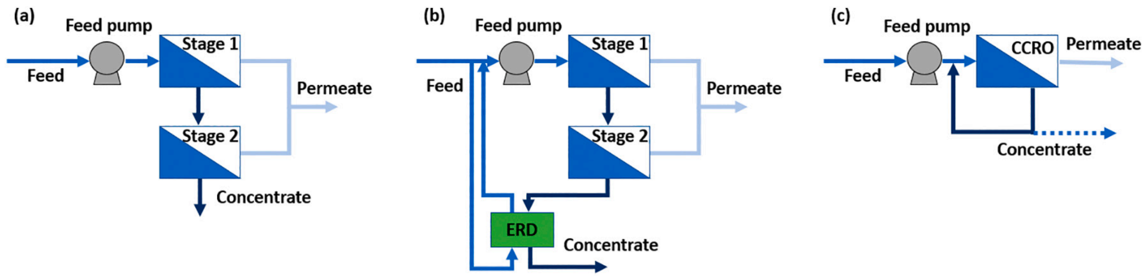

Fig. 1. Diagrams for (a) two-stage RO, (b) two-stage RO with an energy recovery device (ERD), and (c) closed-circuit RO (CCRO).

reduced energy consumption, CCRO may offer better resistance to fouling and scaling and operate at higher average fluxes due to higher crossflow velocities [45,46].

1.5. Previous work and objectives

In our previous study (i.e., Wei et al. [47]), a modeling framework was developed to evaluate synergistic blending of treated wastewater with seawater RO process streams. It was found that potable reuse blending scenarios, where treated wastewater is blended with intake seawater have multiple benefits including reduced energy consumption, reduced seawater intake volume requirements, and reduced discharge volumes compared to scenarios with seawater only as the influent.

In the current research, we consider an inverse scenario: blending higher-salinity streams with wastewater upstream of RO desalination at an AWPF. The higher-salinity streams under consideration include BWRO brine and regional brine interceptor streams in scenarios without and with seawater I&I, where scenarios with seawater I&I include additional salinity from I&I processes that are common in coastal regions. In all cases, the higher-salinity streams can provide an additional treatment-plant influent that has likely undergone filtration (either in the subsurface or at a BWRO facility) and may have lower levels of organic matter and other foulant material than the wastewater they will be blended with. The objective of the current study is to evaluate the additional energy consumed in recovering water from higher-salinity streams blended into AWPF influent and to weigh the benefits of reclaiming this water against the additional energy consumption due to the increased salinity of the influent. We consider opportunities to implement or enhance energy and water recovery using an ERD or CCRO. We also consider whether permeate salinity will meet water quality requirements and whether brine salinity will meet discharge regulations. Recognizing that blending streams with different salinities generates entropy and raises the thermodynamic least work to recover the water, an option of desalinating the higher-salinity streams separately is also considered as well as the inorganic scaling potential associated with treating the streams separately and blended.

2. Methodology

2.1. Flowrates and salinities of treated wastewater, intruded seawater, and higher-salinity streams

All simulations were based on a large AWPF with 5.1×10^5 m^3/day (134 MGD) of secondary-treated wastewater entering the AWPF. 1.5×10^5 m^3/day (40 MGD) of higher-salinity streams were added to mimic the additional influent flowrate required for the OCWD Groundwater Replenishment System to achieve its final expansion capacity. An industry-standard AWPF treatment train with ultrafiltration (UF), RO, and advanced oxidation using UV light coupled with hydrogen peroxide (UV/H_2O_2) processes was modeled for treating the secondary-treated wastewater effluent.

Example salinities of secondary-treated wastewater effluents serving as influent to selected AWPFs are listed in Table S.3. For scenarios without seawater I&I, 1.2 g/L was used as the secondary-treated wastewater effluent (i.e., AWPF influent) salinity. For the seawater I&I scenarios, 2.5, 5, 7.5, and 10% were considered, where the 2.5% seawater I&I scenario assumed a volumetric blending of 2.5% seawater with 97.5% secondary-treated wastewater effluent. Assuming the intruded seawater has a salinity close to that of bulk seawater [48], the world-average salinity of seawater (34.4 g/L [49]) was used as the salinity of intruded seawater. Calculated salinities for the 2.5, 5.0, 7.5, and 10% seawater I&I scenarios were 2.0, 2.8, 3.6, and 4.4 g/L.

Typical salinities of BWRO brines and a regional brine interceptor were used in the simulations. For the BWRO brines, because the salinity of source waters to BWRO facilities can range from 0.5 to 10 g/L with very different ionic compositions [50] and because the water recoveries of BWRO facilities can range from 59 to 90% [38,51,52], three example salinities were selected: 7.5, 10.9, and 17.5 g/L, which represent salinities of typical BWRO brines (e.g., brines in Martinetti [53] and Oren [54]). The regional brine interceptor stream was modeled after a portion of the Inland Empire Brine Line. Although the Inland Empire Brine Line includes industrial wastewater contributions, for the purposes of this research, a brine interceptor that comprises only brines from desalters and ion exchange facilities was modeled; a salinity of 5.7 g/L [33] was used. Ion and constituent concentrations of the treated wastewater, intruded seawater, and higher-salinity streams are summarized in Table S.4. A schematic showing flowrates and salinities of the wastewater, intruded seawater, and higher-salinity streams is shown in Fig. 2. Salinities of the AWPF influent (i.e., the b values in Fig. 2) are the salinity of the blended wastewater, intruded seawater, and higher-salinity stream that are summarized in Table 1.

As shown in Fig. 2, the higher-salinity streams can be blended with the wastewater at two possible locations; depending on their water quality, the higher-salinity streams can be blended 1) into the wastewater reclamation facility influent or 2) into the AWPF influent (bypassing the wastewater reclamation facility). The second combination point has the benefit of avoiding salinity increases in the biological process at the wastewater reclamation facility. According to previous studies (e.g., Linaric [55] and He [56]), when influent salt concentrations are less than 10 g/L NaCl, microorganisms are able to acclimate in several weeks. Uygur [57] also showed that when salinity increases from 0 to 10 g/L, the COD removal rate increases by 25%, but that further increases in salinity cause COD removal rates to decrease. Given that the highest blended wastewater salinity (the highest influent salinity to the biological treatment process) is 7.4 g/L, performance decline in not a significant concern for the biological treatment process.

2.2. Modeling framework

A framework, similar to that developed in our previous study (i.e., Wei et al. [47]) was used. The SEC of the RO process was determined using DOW™ WAVE design software. The RO water-recovery was set to 75% and in order to balance the ratio of permeate flowrate in the lead element to permeate flowrate in the tail element, a hybrid approach (suggested by DuPont Water Solutions [58]) was used. The apprach uses RO membranes with lower water permeability as the lead elements and

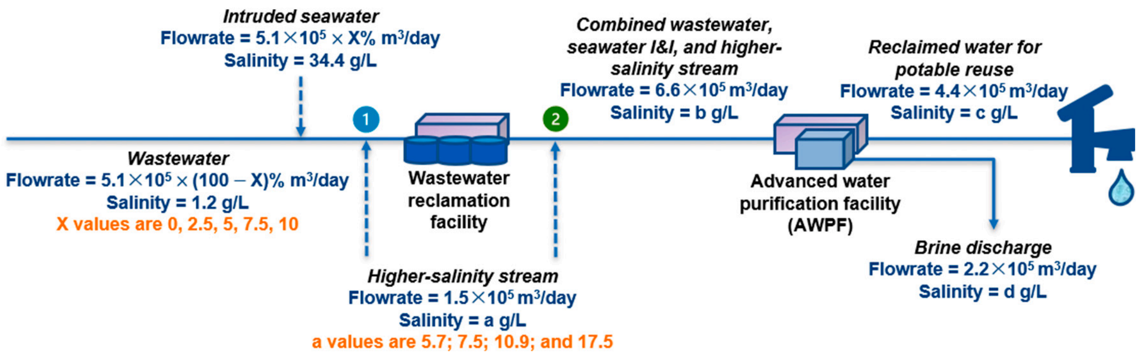

Fig. 2. Schematic of flowrates and salinities for the wastewater, intruded seawater, and higher-salinity streams entering an advanced water purification facility. *X* represents the percentage of seawater I&I; *a* represents the salinity of the higher-salinity stream; *b* represents the influent salinity to the advanced water purification facility (see Table 1); *c* and *d* represent the resulting salinities of the RO permeate and brine streams. There are two possible blending points for the higher-salinity streams (points 1 and 2), selection of which depends on the water quality of the higher-salinity stream. Because wastewater treatment processes generally do not decrease salinity, the choice of blending point does not affect salinity values *b*, *c*, and *d*.

Table 1
Salinities of the advanced water purification facility influent for all scenarios considered. The 25 values shown in the table are used as the *b* value in Fig. 2.

Seawater I&I (%)	Influent salinity without higher-salinity streams (g/L)	Influent salinity with brine interceptor (g/L)	Influent salinity with BWRO brine 1 (g/L)	Influent salinity with BWRO brine 2 (g/L)	Influent salinity with BWRO brine 3 (g/L)
0	1.2	2.2	2.6	3.4	4.9
2.5	2.0	2.9	3.3	4.1	5.6
5	2.8	3.5	3.9	4.7	6.2
7.5	3.6	4.1	4.5	5.3	6.8
10	4.4	4.7	5.1	5.9	7.4

RO membranes with higher water permeabilities as the tail elements. The RO system was simulated with 24 trains, with each train having a two-stage RO array. In stages 1 and 2, there were 103 and 55 vessels, with each vessel containing four BW30XFR-400/34i membrane elements as the lead elements and four BW30XFRLE-400/34i membrane elements as the tail elements. Both RO membranes are from DuPont Water Solutions (Edina, MN) and are suitable for both potable water reuse and industrial water demineralization. Because increasing influent salinity can shift operating windows [59], the back pressure applied to the permeate stream in stage 1 and the booster pressure applied to the feed stream in stage 2 were adjusted and are summarized in Table S.5. Values for Langelier Saturation Index (LSI), percent saturation of $CaSO_4$, and percent saturation of SiO_2 were calculated by the software alongside flowrate and energy values.

Simulations of the UF pretreatment process and UV/H_2O_2 advanced oxidation process were adapted from our previous study (i.e., Wei et al. [47]). Given that the seawater I&I and higher-salinity brine streams have likely undergone filtration (either in the subsurface or at a BWRO facility), it is assumed that blending the higher-salinity streams into the UF feed will not significantly affect the energy required by the UF or UV/H_2O_2 processes. The UF process was simulated with 90% water recovery using WAVE design software; the *SEC* per cubic meter of UF filtrate ($SEC_{UF-filtrate}$) was determined to be 0.09 kWh/m^3. The *SEC* of the UF process per cubic meter of product water (SEC_{UF}) was determined to be 0.11 kWh/m^3. A UV dose of 900 mJ/cm^2 was simulated for treating the RO permeate. At this dose, the *SEC* of the UV/H_2O_2 process per cubic meter of product water (SEC_{UV/H_2O_2}) is 0.13 kWh/m^3 [47].

SEC values for UF, RO, and UV/H_2O_2 are summed as SEC_{Net}. For scenarios not using an ERD, SEC_{Net} is calculated as:

$$SEC_{Net} = SEC_{UF} + SEC_{RO} + SEC_{UV/H_2O_2} \quad (1)$$

In simulations where an ERD is implemented, the specific energy saving (*SES*) was determined using:

$$SES = \frac{P_{brine} \times F_{brine}}{F_{permeate}} \quad (2)$$

where P_{brine} is hydraulic pressure of the RO brine, F_{brine} is flowrate of the RO brine, and $F_{permeate}$ is RO permeate flowrate. SEC_{Net} for these simulations was calculated as:

$$SEC_{Net} = SEC_{UF} + SEC_{RO} + SEC_{UV/H_2O_2} - SES \quad (3)$$

All *SEC* and *SES* values are in units of kWh per cubic meter of product water.

The CCRO process was simulated using DOW™ WAVE design software with water-recovery set both at 75% for comparison with two-staged RO and at 85% to simulate a more common recovery rate for CCRO applications. The CCRO process was simulated with 24 trains, each having a one-stage RO array and 181 vessels, with each vessel containing two FilmTec™ SOAR-5000 membrane elements as the lead elements and five FilmTec™ SOAR-4000 membrane elements as the tail elements. SEC_{Net} for CCRO was calculated using Eq. (1).

2.3. Separate desalination of higher-salinity streams and inorganic scaling potential associated with treating the streams separately and blended

If the higher-salinity streams are desalinated in a separate RO train and not in the AWPF RO train, it may be desirable to operate the separate RO processes at a different water recovery than the AWPF RO process (shown in Table S.6). In order to achieve an overall 75% recovery (and provide the additional water supply of 1.5×10^5 m^3/day (40 MGD)), the relationship between the two water recoveries can be formulated as:

$$WR_{ww} \times 134\ MGD + WR_{hss} \times 40\ MGD = 75\% \times 174\ MGD \quad (4)$$

where WR_{ww} is RO water recovery for the treated wastewater, and WR_{hss} is RO water recovery for the higher-salinity stream. WAVE design software was then used to separately determine SEC_{Net} for the treated wastewater (SEC_{Net_ww}) and SEC_{Net} for the higher-salinity stream (SEC_{Net_hss}). The combined SEC_{Net} was calculated using:

$$SEC_{Net} = \frac{SEC_{Net\_ww} \times WR_{ww} \times 134\ MGD + SEC_{Net\_hss} \times WR_{hss} \times 40\ MGD}{75\% \times 174\ MGD} \quad (5)$$

Given the high concentration of some ionic constituents in the higher-salinity streams (Table S.4) inorganic scaling may be a limiting factor in water recovery [60]. Scaling of $CaCO_3$, $CaSO_4$ and SiO_2 is considered because these are the most common sparingly soluble salts in RO systems [58,61–64]. LSI is used as an indicator of $CaCO_3$ scaling because LSI is appropriate for influent salinities less than 10 g/L. Percent saturation is used as an indicator of $CaSO_4$ and SiO_2 scaling. LSI values span from negative to positive values with negative values indicating less potential for $CaCO_3$ scaling; percent saturation values span from 0 to 100 with lower values indicating less potential for scaling [65]. The scaling indicators are compared for two cases: when the higher-salinity streams are blended with the treated wastewater and when the higher-salinity streams are desalinated separately.

3. Results and discussion

3.1. Effect of seawater I&I and higher-salinity streams on SEC_{Net} and permeate and brine discharge salinities

Values of SEC_{Net} without and with higher-salinity streams were calculated and the results are shown in Fig. 3. The conditions without higher-salinity streams, given by the first bar of each group and the red horizontal line, represent the base cases for the five seawater I&I scenarios. At 0% seawater I&I, the base case SEC_{Net} (the first bar of the first group) is 0.54 kWh/m^3. As the higher-salinity streams are considered (the next four bars of the first group), SEC_{Net} increases with increasing stream salinity. Comparing base case SEC_{Net} values for the five scenarios (the first bar of each group), it can be seen that SEC_{Net} increases from 0.54 to 0.87 kWh/m^3 as seawater I&I increase from 0 to 10%. This range is consistent with previous research on energy consumption in RO-based water reuse (e.g., 0.76 kWh/m^3 from Holloway et al. [66]). As base case SEC_{Net} increases with increasing seawater I&I, the percent increase of SEC_{Net} caused by mixing higher-salinity streams decreases. In other words, for the 10% seawater I&I base case (the first bar of the last group), SEC_{Net} is 0.87 kWh/m^3 and when BWRO brine 3 is added (the last bar of the last group), SEC_{Net} is 1.17 kWh/m^3. This is only a 34% increase compared to the 69% increase in SEC_{Net} for the 0% seawater I&I case. From Fig. 4, it can be seen that the percent increase of SEC_{Net} caused by mixing higher-salinity streams ($\Delta SEC_{Net}/\Delta Salinity = \frac{SEC_{Net\ with\ higher-salinity\ stream} - SEC_{Net\ without\ higher-salinity\ stream}}{Salinity_{Higher-salinity\ stream} - Salinity_{Treated\ wastewater}}$) is lower for the less saline streams and decreases as seawater I&I increases. Looking to the future, base case salinity is expected to continue increasing [67,68] and as it does, the reduced percent increase of SEC_{Net} will bring greater value to utilizing the water resource in higher-salinity streams.

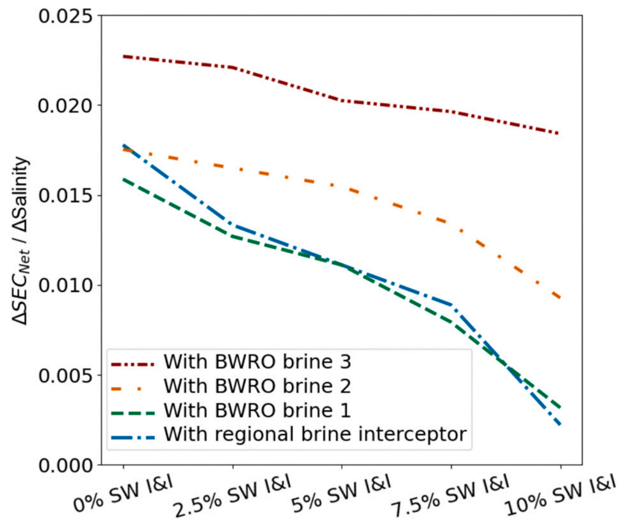

Fig. 4. Percent increase of SEC_{Net} caused by mixing higher-salinity streams. The percent increase of SEC_{Net} is generally lower for less saline streams; the percent increase of SEC_{Net} decreases as seawater I&I increases for all higher-salinity streams.

Permeate salinities for the five seawater I&I scenarios are shown in Fig. 5a (and values are given in Table S.7). All permeate salinities are less than the US Environmental Protection Agency secondary-treated wastewater effluent standard of 500 mg/L TDS and are expected to be less than most water quality regulations (e.g., the limit of salinity in recycled water recharged into the OCWD groundwater basin is 580 mg/L) [34]. Brine discharge salinities are shown in Fig. 5b (and values are given in Table S.8). All brine discharge salinities are less than typical discharge salinity limits to the ocean, which are often set at an increment (e.g., 1 part per thousand) above ambient or at an absolute level (e.g., 40 g/L) [69].

3.2. SEC_{Net} when using RO-ERD

To determine whether the *SES* from an ERD can compensate for the additional RO energy required from higher-salinity streams, Fig. 6 shows values of SEC_{Net} without using an ERD (the left-hand bar of each

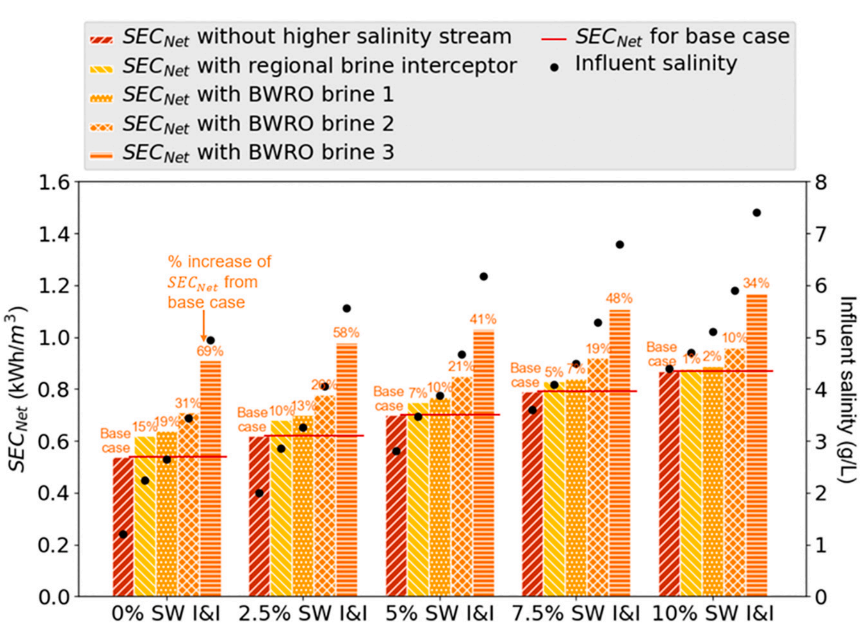

Fig. 3. SEC_{Net} without and with higher-salinity streams for the five seawater I&I scenarios. The first bar in each group represents the SEC_{Net} for advanced water purification facilities without adding higher-salinity streams (the base case). The other four bars in each group represent the SEC_{Net} for facilities with higher-salinity streams. The red horizontal lines represent the base case SEC_{Net} for each group and the black dots represent the influent salinity. All values are for systems without ERDs or CCRO. (For interpretation of the references to colour in this figure legend, the reader is referred to the web version of this article.)

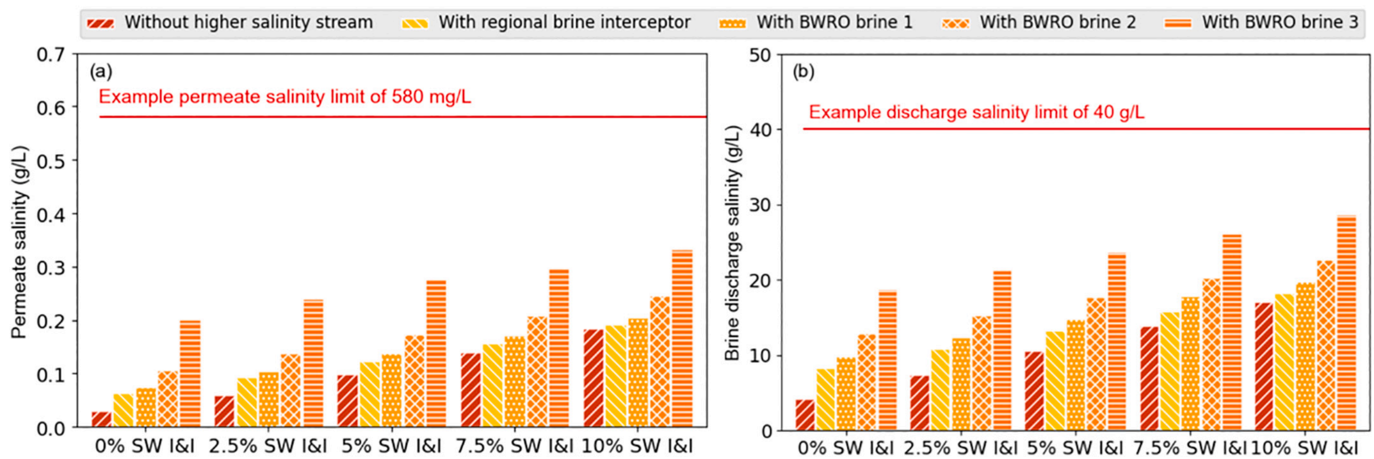

Fig. 5. Salinity values for a) permeate and b) brine discharge without and with higher-salinity streams for the five seawater I&I scenarios. The red horizontal lines represent example permeate and discharge regulatory limits. (For interpretation of the references to colour in this figure legend, the reader is referred to the web version of this article.)

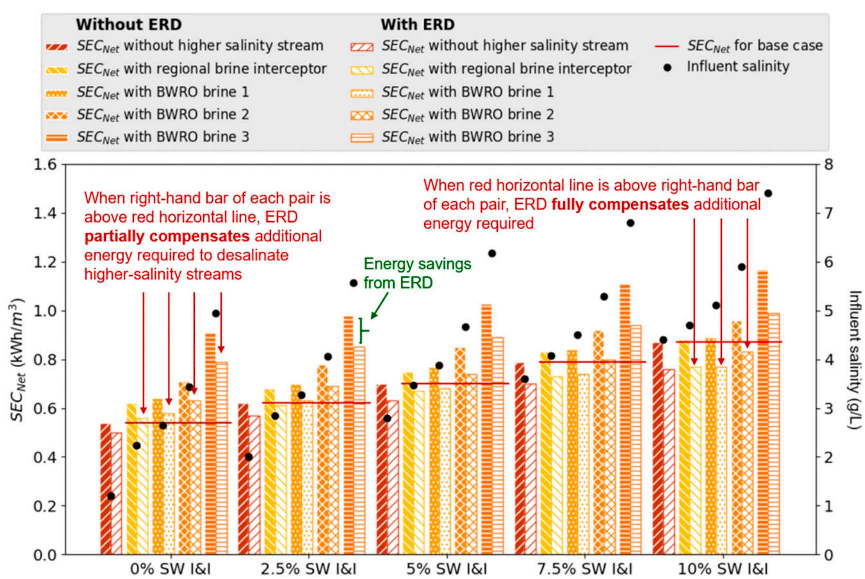

Fig. 6. SEC_{Net} without and with higher-salinity streams for the five seawater I&I scenarios. Bars are paired with the left-hand bar representing SEC_{Net} for advanced water purification facilities without an ERD and the right-hand bar representing SEC_{Net} for facilities with an ERD. The difference between the left-hand and right-hand bars represents the energy savings from an ERD. The first pair of bars in each group represents SEC_{Net} for the base case of each group and the red horizontal line allows comparison of the base case of each group with the higher-salinity cases. The black dots represent the influent salinity for each pair. (For interpretation of the references to colour in this figure legend, the reader is referred to the web version of this article.)

pair) alongside values of SEC_{Net} when using an ERD (the right-hand bar of each pair); the difference between the left-hand and right-hand bars represent the *SES* provided by an ERD. At 0% seawater I&I percentage for the base case (the first pair of the first group), *SES* is 0.04 kWh/m^3. Comparison of *SES* values for the base cases of the five scenarios (the difference between the left-hand and right-hand bars of the first pair of each group), shows that as seawater I&I increases from 0 to 10%, *SES* increases from 0.04 to 0.11 kWh/m^3. With increasing salinity of the higher-salinity streams, the *SES* from using an ERD increases as well.

For all scenarios, when the SEC_{Net} for RO-ERD (the right-hand bar of each pair) is above the red horizontal line, it indicates that the ERD partially compensates for the additional SEC_{Net} required to desalinate the higher-salinity influent. For example, at 0% seawater I&I, the *SES* from an ERD partially (32–75%) compensates for the additional SEC_{Net} caused by higher-salinity streams. When the red horizontal line is above the SEC_{Net} for RO-ERD (the right-hand bar of each pair), the *SES* from an ERD fully compensates for the additional energy required to desalinate the higher-salinity influent. At 10% seawater I&I, the *SES* from an ERD fully compensates the additional $SEC_{Net}$when the brine interceptor, BWRO brine 1, and BWRO brine 2 are the higher-salinity streams. When BWRO brine 3 is the higher-salinity streams, the *SES* from an ERD partially (60%) compensates for the additional energy required to desalinate the higher-salinity influent. Thus, for some scenarios the influent can be augmented (and the brine stream used beneficially) without additional energy consumption simply by implementing an ERD. In the future, as higher applied pressures are required to overcome the higher osmotic pressures of more saline feed streams, greater hydraulic energy can be recovered from the brine stream and the *SES* from ERDs will increase. However, achieving energy savings might not be sufficient to warrant the addition of an ERD to AWPF RO systems; the capital cost of the ERD, as well as maintenance costs, must be considered in decision-making.

3.3. SEC_{Net} when using CCRO

As mentioned earlier, CCRO systems are being considered at AWPFs to improve water recovery while keeping energy consumption low. To determine whether the *SES* from CCRO can compensate for the additional RO energy required from higher-salinity streams at the same RO water recovery rates as used in previous sections (75%), Fig. 7 shows values of SEC_{Net} using regular RO (the left-hand bar of each pair) and values of SEC_{Net} using CCRO at 75% recovery rate (the right-hand bar of

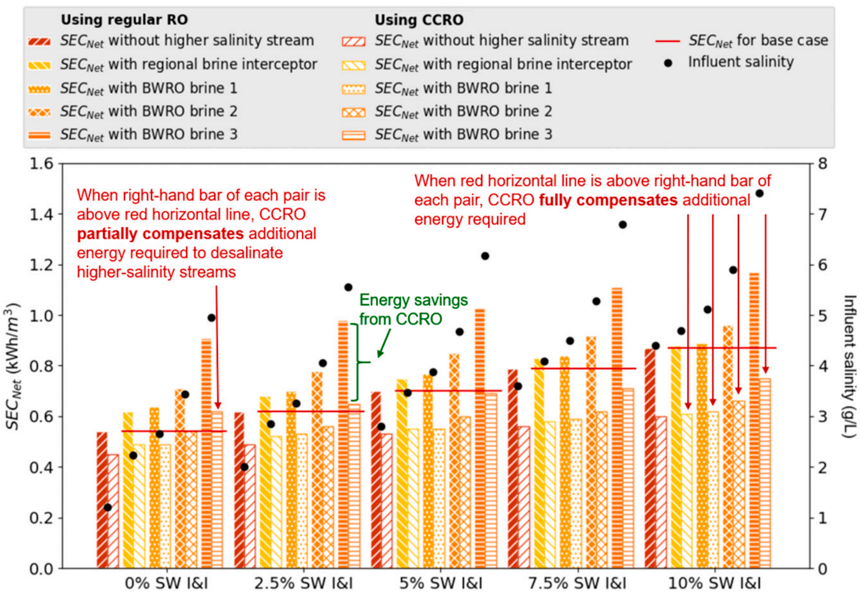

Fig. 7. SEC_{Net} without and with higher-salinity streams for the five seawater I&I scenarios. Bars are paired with the left-hand bar representing SEC_{Net} for advanced water purification facilities using regular RO and the right-hand bar representing the SEC_{Net} for facilities using CCRO. The difference between the left-hand and right-hand bars represents the energy savings from CCRO. The first pair of bars in each group represents the SEC_{Net} for the base case of each group and the red horizontal line allows comparison of the base case of each group with other cases that represent addition of higher-salinity streams. The black dots represent influent salinity for each pair.

each pair); the difference between the left-hand and right-hand bars represent the *SES* provided by CCRO. At 0% seawater I&I percentage for the base case (the first pair of the first group), *SES* is 0.09 kWh/m^3. Comparing *SES* values for the base cases of the five scenarios (the difference between the left-hand and right-hand bars of the first pair of bars of each group), shows that as seawater I&I increases from 0 to 10%, *SES* increases from 0.09 to 0.27 kWh/m^3. With increasing salinity of the higher-salinity streams, the *SES* from CCRO increases as well. For all scenarios, when the SEC_{Net} for CCRO (the right-hand bar of each pair) is above the red horizontal line, it indicates that the CCRO partially compensates for the additional SEC_{Net} required to desalinate the higher-salinity influent. For example, at 0% seawater I&I, when BWRO brine 3 is the higher-salinity stream, the *SES* from CCRO partially (78%) compensates for the additional SEC_{Net} caused by the higher-salinity stream. When the red horizontal line is above the SEC_{Net} for CCRO (the right-hand bar of each pair), the *SES* from CCRO fully compensates for the additional energy required to desalinate the higher-salinity influent. At 10% seawater I&I, the *SES* from CCRO fully compensates the additional SEC_{Net}. Clearly, there are energetic benefits to implementing CCRO; however, retrofitting the current RO system to CCRO will require additional capital and operating costs, especially regarding the control of variable pressures [70].

Perhaps more important than energy savings from CCRO, the possibility of operating CCRO at a higher recovery was also considered. Values of SEC_{Net} for CCRO at 85% recovery are shown in Fig. S.1 alongside values for CCRO at 75% recovery. The simulations indicate that increasing CCRO recovery rate from 75 to 85% increases the SEC_{Net} by 8 to 10%, which is an increase of approximately 0.02 to 0.04 kWh/m^3.

Permeate and brine discharge salinities for CCRO at 85% recovery are shown in Fig. 8. In all cases except one, the permeate salinities (Fig. 8a) are less than the example permeate salinity limit of 580 mg/L (i.e., the limit of salinity in recycled water recharged into the OCWD groundwater basin). For the most saline stream (when seawater I&I is 10% and when BWRO brine 3 is the higher-salinity stream), the permeate salinity (656 mg/L) exceeds the example salinity limit. Brine discharge salinities (Fig. 8b) exceed the example brine discharge limit of 40 g/L in two cases. For the most saline streams, the brine discharge salinities are 42 and 46 g/L. Even though the SEC_{Net}, permeate salinity, and brine discharge salinity are higher when operating CCRO at 85% recovery, the decreased brine discharge flowrate (see values in Fig. S.2) may be important if zero liquid discharge becomes a goal.

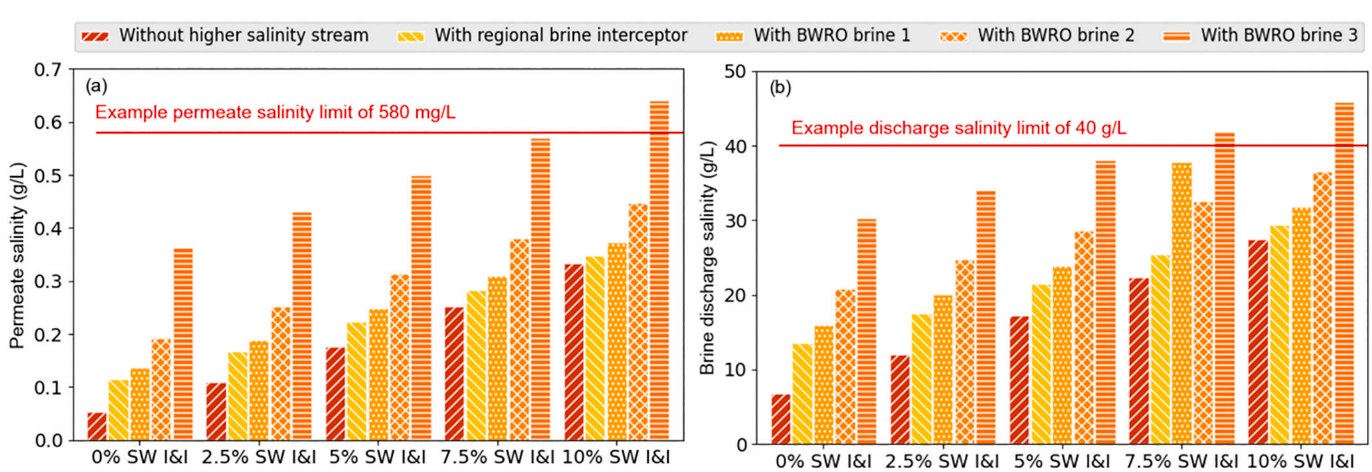

Fig. 8. Salinity values for a) permeate and b) brine discharge when CCRO at 85% recovery is used for all scenarios. The red horizontal lines represent example permeate and discharge regulatory limits. (For interpretation of the references to colour in this figure legend, the reader is referred to the web version of this article.)

3.4. Separate desalination of higher-salinity streams and inorganic scaling potential associated with treating the streams separately and blended

Energy savings from separate desalination was quantified (Fig. S.3) and separate desalination was found to not be competitive with blended desalination using ERD or CCRO (Fig. S.4). LSI values, percent saturation of $CaSO_4$, and percent saturation of SiO_2 of the RO brine discharge when desalinating the higher-salinity streams separately from the treated wastewater and when desalinating the treated wastewater and higher-salinity streams together are shown in Table S.9–11. RO recovery rate was 75% for all streams. $CaCO_3$ scaling is indicated for the regional brine interceptor, BWRO brine 1, and BWRO brine 3 as well as for the treated wastewater (Table S.9). For the blended influent, the LSI values range from 1.3 to 1.8, which are not substantially higher than the range of LSI values for the treated wastewater alone (1.0 to 1.3). In a study by Drak et al. [71], four antiscalants were found to enableRO recovery levels equal to or exceeding 88% when LSI levels exceeding 2.0. Thus, the small increase in $CaCO_3$ scaling potential due to blending can likely be addressed by the existing antiscalant. $CaSO_4$ scaling is indicated for all of the higher-salinity streams but not for the treated wastewater (Table S.10). For the blended influent, percent saturation values are below 100% for the regional brine interceptor and BWRO brine 3 (ranging from 68 to 80%) but exceed 100% for BWRO brines 1 and 2 (ranging from 110 to 140%). A change in the antiscalant recipe – or other upstream treatment [72], – is likely necessary to address $CaSO_4$ scaling concerns when BWRO brines 1 and 2 are blended and perhaps when the regional brine interceptor and BWRO brine 3 are blended as well. SiO_2 scaling is indicated for all the higher-salinity streams and perhaps for the treated wastewater as well (saturation values range from 67 to 95%) (Table S.11). For the blended influent, percent saturation values range from 88 to 139%; this increase in SiO_2 scaling potential due to blending can likely be addressed by an adjustment to the existing antiscalant.

In summary, preliminary assessment of scaling potentials shows that blending decreases the scaling potentials of $CaCO_3$, $CaSO_4$, and SiO_2 compared to when the higher-salinity streams are desalinated separately but increases scaling potential compared to the treated wastewater alone. From the perspective of desalinating the blended streams, higher antiscalant dosages may be required and in the case of CaSO4, additional treatment may be desired; in all cases, operation and maintenance costs for chemicals and cleaning in place are likely to increase [73]. From the perspective of whether to treat the higher-salinity streams separately or blended with treated wastewater, there is clear benefit in the dilution provided by blending.

3.5. Conclusions and implications

Higher-salinity streams can provide an additional treatment-plant influent that has undergone pretreatment. This framework considers how ERDs and CCRO can mitigate the additional energy required to desalinate the higher-salinity influent; however, instead of considering the value of ERDs and CCRO from the standpoint of energy savings alone, this analysis also considers the additional salinity that can be treated, which may have greater value than energy reduction at AWPFs. The energy savings is shown to be greater for CCRO than for RO-ERD and the energy savings is shown to increase for both as influent salinity increases. CCRO can achieve higher recoveries (e.g., 85%) whereas RO-ERD is limited by low brine flowrates at higher recoveries. Addition of higher-salinity streams was also considered within the context of permeate water quality requirements and discharge regulations that may limit recoveries. Although higher-salinity streams likely have lower levels of organics and other membrane foulants, they often have higher levels of inorganic scalants. Adjusted antiscalant doses may be needed for the blended streams; on the other hand, blending (dilution) is beneficial for recovery of water from the higher-salinity streams. In the future, capital and operating costs should be considered as well as enhanced source control that ensures known water quality of the feed stream. Given that water conservation and seawater I&I have already resulted in more saline influents, the percent increase of energy consumption decreases with blending of higher-salinity streams. And given that this cycle is exacerbated by climate change, the additional energy cost of introducing more salinity into potable reuse systems is expected to have a decreasing trend in future years.

CRediT authorship contribution statement

Xin Wei: methodology, investigation, visualization, validation, writing

Kelly Sanders: visualization, validation, reviewing

Amy Childress: conceptualization, methodology, investigation, visualization, writing, supervision, reviewing

Declaration of competing interest

The authors declare that they have no known competing financial interests or personal relationships that could have appeared to influence the work reported in this paper.

Acknowledgement

We acknowledge support from the University of Southern California's Theodore and Wen-Hui Chen Endowed Fellowship and the University of Southern California's Viterbi/Graduate School Ph.D. Fellowship to X. Wei. We thank Jason Dadakis from Orange County Water District (OCWD) and Lan Wiborg and Mark Kawamoto from Orange County Sanitation District (OCSD) for useful information regarding operation details at OCWD and OCSD. We also thank Jeff Mosher from Santa Ana Watershed Project Authority, Kevin Alexander from Hazen and Sawyer and Bob Ohlund from Dudek for providing valuable insight and feedback on this manuscript.

Appendix A. Supplementary data

Supplementary data to this article can be found online at https://doi.org/10.1016/j.desal.2021.115316.

References

[1] US Environmental Protection (US EPA), National Water Reuse Action Plan - Improving the security, sustainability, and resilience of our nation's water resources, Available: https://www.epa.gov/sites/production/files/2020-02/documents/national-water-reuse-action-plan-collaborative-implementation-version-1.pdf, 2020.

[2] G. Tchobanoglous, et al., Framework for Direct Potable Reuse, WateReuse Research Foundation, 2015.

[3] Bluefield Research, U.S. Municipal Wastewater & Reuse: Market Trends, Opportunities and Forecasts, 2015-2025, Insight Reports Water Reuse, 2015.

[4] US Environmental Protection (US EPA), Potable reuse compendium, Available: https://www.epa.gov/sites/production/files/2018-01/documents/potablereusecompendium_3.pdf?TB_iframe=true&width=370.8&height=658.8, 2018.

[5] Singapore National Water Agency, NEWater, Available at: https://www.pub.gov.sg/watersupply/fournationaltaps/newater, 2021.

[6] M. Kurihara, M. Hanakawa, Mega-ton water system: japanese national research and development project on seawater desalination and wastewater reclamation, Desalination 308 (2013) 131–137.

[7] F. Tang, et al., Fouling of reverse osmosis membrane for municipal wastewater reclamation: autopsy results from a full-scale plant, Desalination 349 (2014) 73–79.

[8] M.F. Hamoda, N.F. Attia, I.A. Al-Ghusain, Performance evaluation of a wastewater reclamation plant using ultrafiltration and reverse osmosis, Desalin. Water Treat. 54 (2015) 2928–2938.

[9] S.D. Lyu, W.P. Chen, W.L. Zhang, Y.P. Fan, W.T. Jiao, Wastewater reclamation and reuse in China: opportunities and challenges, J. Environ. Sci. 39 (2016) 86–96.

[10] F. Tang, et al., Fouling characteristics of reverse osmosis membranes at different positions of a full-scale plant for municipal wastewater reclamation, Water Res. 90 (2016) 329–336.

[11] I.G. Wenten, Khoiruddin, reverse osmosis applications: prospect and challenges, Desalination 391 (2016) 112–125.

[12] California State Water Resources Control Board, Regulations Related to Recycled Water - Title 22 code of regulations, Available: https://www.waterboards.ca.gov/drinking_water/certlic/drinkingwater/documents/lawbook/rwregulations_20181001a.pdf, 2018.

[13] T. Zeng, M.J. Plewa, W.A. Mitch, N-nitrosamines and halogenated disinfection byproducts in US full advanced treatment trains for potable reuse, Water Res. 101 (2016) 176–186.

[14] A.A. Alturki, et al., Combining MBR and NF/RO membrane filtration for the removal of trace organics in indirect potable water reuse applications, J. Membr. Sci. 365 (2010) 206–215.

[15] T. Wintgens, et al., The role of membrane processes in municipal wastewater reclamation and reuse, Desalination 178 (2005) 1–11.

[16] R.P. Lively, D.S. Sholl, From water to organics in membrane separations, Nat. Mater. 16 (2017) 276–279.

[17] A.K. Venkatesan, S. Ahmad, W. Johnson, J.R. Batista, Systems dynamic model to forecast salinity load to the Colorado River due to urbanization within the Las Vegas Valley, Sci. Total Environ. 409 (2011) 2616–2625.

[18] K. Sardari, P. Fyfe, D. Lincicome, S.R. Wickramasinghe, Combined electrocoagulation and membrane distillation for treating high salinity produced waters, J. Membr. Sci. 564 (2018) 82–96.

[19] K. Schwabe, M. Nemati, R. Amin, Q. Tran, D. Jassby, Unintended consequences of water conservation on the use of treated municipal wastewater, Nature Sustainability 3 (2020) 628–635.

[20] Available (2011). https://your.kingcounty.gov/dnrp/library/wastewater/cso/docs/2011-03_SaltwaterIntrusionAndInfiltrationStudy.pdf.

[21] S.A. Krayer, I.M. Michaels, P.T. Solomon, Salinity Impacts on Coastal Wastewater Treatment Facilities, A Major Qualifying Project Report - Degree of Bachelor of Science, 2017.

[22] D.M. Warsinger, et al., A review of polymeric membranes and processes for potable water reuse, Prog. Polym. Sci. 81 (2018) 209–237.

[23] D. Gerrity, B. Pecson, R.S. Trussell, R.R. Trussell, Potable reuse treatment trains throughout the world, J. Water Supply Res Technol. 62 (2013) 321–338.

[24] M. Al-Obaidi, C. Kara-Zaitri, I.M. Mujtaba, Wastewater Treatment by Reverse Osmosis Process: State of the Art & Process Modelling, CRC Press, 2020.

[25] V. Lazarova, et al., Production of high quality water for reuse purposes: the West Basin experience, in: 3rd World Water Congress Efficient Water Supply and Water Reuse 3, 2003, pp. 167–175.

[26] B.K. Pramanik, L. Shu, V. Jegatheesan, A review of the management and treatment of brine solutions, Environ. Sci.: Water Res. Technol. 3 (2017) 625–658.

[27] S. Lee, Y. Kim, A.S. Kim, S. Hong, Evaluation of membrane-based desalting processes for RO brine treatment, Desalin. Water Treat. 57 (2016) 7432–7439.

[28] A.K. Fard, T. Rhadfi, M. Khraisheh, M.A. Atieh, N. Hilal, Reducing flux decline and fouling of direct contact membrane distillation by utilizing thermal brine from MSF desalination plant, Desalination 379 (2016) 172–181.

[29] X. Ji, et al., Membrane distillation-crystallization of seawater reverse osmosis brines, Sep. Purif. Technol. 71 (2010) 76–82.

[30] A. Panagopoulos, K.J. Haralambous, M. Loizidou, Desalination brine disposal methods and treatment technologies - a review, Sci. Total Environ. 693 (2019) 23.

[31] W.S. Walker, Improving Recovery in Reverse Osmosis Desalination of Inland Brackish Groundwaters via Electrodialysis, Available:, Doctoral dissertation at the University of Austin at Texas, 2010 https://repositories.lib.utexas.edu/handle/2152/ETD-UT-2010-08-1693.

[32] N. Voutchkov, Energy use for membrane seawater desalination - current status and trends, Desalination 431 (2018) 2–14.

[33] Santa Ana Watershed Project Authority (SAWPA), Brine Line Mapping Tools, Available from: https://www.sawpa.net/sari/sari.htm, 2021.

[34] S. Scott-Roberts, Engineer's report for the groundwater replenishment system final expansion projects, Available from: https://www.ocwd.com/media/5234/gwrs-fe-engineers-report-complete.pdf, 2016.

[35] J. Kim, K. Park, S. Hong, Optimization of two-stage seawater reverse osmosis membrane processes with practical design aspects for improving energy efficiency, J. Membr. Sci. 601 (2020) 11.

[36] K. Park, J. Kim, D.R. Yang, S. Hong, Towards a low-energy seawater reverse osmosis desalination plant: a review and theoretical analysis for future directions, J. Membr. Sci. 595 (2020).

[37] A. Zohrabian, S.L. Plata, D. Kim, A.E. Childress, K.T. Sanders, Leveraging the water-energy nexus to derive benefits for the electric grid through demand-side management in the water supply and wastewater sectors, WIREs Water 8 (2021) 1510–1532.

[38] H. Nassrullah, S.F. Anis, R. Hashaikeh, N. Hilal, Energy for desalination: a state-of-the-art review, Desalination 491 (2020) 44.

[39] M.H. Li, Optimal plant operation of brackish water reverse osmosis (BWRO) desalination, Desalination 293 (2012) 61–68.

[40] J. Jeon, et al., Study on the necessity of energy recovery device in small scale reverse osmosis desalination plant, Korean Chem. Eng. Res. 55 (2017) 762–766.

[41] N. Liu, Z.L. Liu, Y.X. Li, L.X. Sang, Development and experimental studies on a fully-rotary valve energy recovery device for SWRO desalination system, Desalination 397 (2016) 67–74.

[42] E. Kadaj, R. Bosleman, Energy recovery devices in membrane desalination processes, in: Renewable Energy Powered Desalination Handbook, 2018, pp. 415–444.

[43] A. Drak, M. Adato, Energy recovery consideration in brackish water desalination, Desalination 339 (2014) 34–39.

[44] D.M. Warsinger, E.W. Tow, K.G. Nayar, L.A. Maswadeh, J.H. Lienhard, Energy efficiency of batch and semi-batch (CCRO) reverse osmosis desalination, Water Res. 106 (2016) 272–282.

[45] R.L. Stover, Industrial and brackish water treatment with closed circuit reverse osmosis, Desalin. Water Treat. 51 (2013) 1124–1130.

[46] R.L. Stover, High recovery, low fouling, and low energy reverse osmosis, Desalin. Water Treat. 57 (2016) 26501–26506.

[47] X. Wei, Z.M. Binger, A. Achilli, K.T. Sanders, A.E. Childress, A modeling framework to evaluate blending of seawater and treated wastewater streams for synergistic desalination and potable reuse, Water Res. 170 (2020) 11.

[48] S. Stein, et al., Saline groundwater from coastal aquifers as a source for desalination, Environ. Sci. Technol. 50 (2016) 1955–1963.

[49] Ocean Health, Detailed composition of seawater at 3.5% salinity, Available: https://oceanplasma.org/documents/chemistry.html, 2020.

[50] N. Voutchkov, Membrane desalination—process selection, design, and implementation, in: Sustainable Desalination Handbook, 2018, pp. 3–24.

[51] A. Altaee, N. Hilal, High recovery rate NF-FO-RO hybrid system for inland brackish water treatment, Desalination 363 (2015) 19–25.

[52] M.A. Alghoul, P. Poovanaesvaran, K. Sopian, M.Y. Sulaiman, Review of brackish water reverse osmosis (BWRO) system designs, Renew. Sustain. Energy Rev. 13 (2009) 2661–2667.

[53] C.R. Martinetti, A.E. Childress, T.Y. Cath, High recovery of concentrated RO brines using forward osmosis and membrane distillation, J. Membr. Sci. 331 (2009) 31–39.

[54] Y. Oren, et al., Pilot studies on high recovery BWRO-EDR for near zero liquid discharge approach, Desalination 261 (2010) 321–330.

[55] M. Linaric, M. Markic, L. Sipos, High salinity wastewater treatment, Water Sci. Technol. 68 (2013) 1400–1405.

[56] H.J. He, et al., Influence of salinity on microorganisms in activated sludge processes: a review, Int. Biodeterior. Biodegradation 119 (2017) 520–527.

[57] A. Uygur, Specific nutrient removal rates in saline wastewater treatment using sequencing batch reactor, Process Biochem. 41 (2006) 61–66.

[58] DuPont Water Solutions, Available: https://www.dupont.com/content/dam/dupont/amer/us/en/water-solutions/public/documents/en/45-D01504-en.pdf, 2021.

[59] A. Ruiz-Garcia, I. Nuez, D. Carrascosa-Chisvert, J.J. Santana, Simulations of BWRO systems under different feedwater characteristics. Analysis of operation windows and optimal operating points, Desalination 491 (2020).

[60] A.J. Karabelas, S.T. Mitrouli, M. Kostoglou, Scaling in reverse osmosis desalination plants: a perspective focusing on development of comprehensive simulation tools, Desalination 474 (2020) 18.

[61] D.M. Warsinger, et al., Inorganic fouling mitigation by salinity cycling in batch reverse osmosis, Water Res. 137 (2018) 384–394.

[62] H.J. Lee, M.A. Halali, T. Baker, S. Sarathy, C.F. de Lannoy, A comparative study of RO membrane scale inhibitors in wastewater reclamation: antiscalants versus pH adjustment, Sep. Purif. Technol. 240 (2020).

[63] H.L. Yang, C. Huang, J.R. Pan, Characteristics of RO foulants in a brackish water desalination plant, Desalination 220 (2008) 353–358.

[64] S. Mitrouli, A.J. Karabelas, A. Karanasiou, M. Kostoglou, Incipient calcium carbonate scaling of desalination membranes in narrow channels with spacers-experimental insights, J. Membr. Sci. 425 (2013) 48–57.

[65] A. Antony, et al., Scale formation and control in high pressure membrane water treatment systems: A review, J. Membr. Sci. 383 (2011) 1–16.

[66] R.W. Holloway, et al., Life-cycle assessment of two potable water reuse technologies: MF/RO/UV-AOP treatment and hybrid osmotic membrane bioreactors, J. Membr. Sci. 507 (2016) 165–178.

[67] K.M. Befus, P.L. Barnard, D.J. Hoover, J.A.F. Hart, C.I. Voss, Increasing threat of coastal groundwater hazards from sea-level rise in California, Nature, Clim. Chang. 10 (2020) 946.

[68] M.A. Hummel, M.S. Berry, M.T. Stacey, Sea level rise impacts on wastewater treatment systems along the US coasts, Earths Future 6 (2018) 622–633.

[69] S. Jenkins, J. Paduan, P.J.W. Roberts, D. Schlenk, J. Weis, Management of Brine Discharges to Coastal Waters Recommendations of a Science Advisory Panel, Southern California Coastal Water Research Project, Costa Mesa, CA, 2012.

[70] J.R. Werber, A. Deshmukh, M. Elimelech, Can batch or semi-batch processes save energy in reverse-osmosis desalination? Desalination 402 (2017) 109–122.

[71] A. Drak, et al., Laboratory technique for predicting the scaling propensity of RO feed waters, Desalination 132 (2000) 233–242.

[72] DuPont Water Solutions, Available: https://www.dupont.com/content/dam/dupont/amer/us/en/water-solutions/public/documents/en/45-D01553-en.pdf, 2021.

[73] A. Ruiz-Garcia, J. Feo-Garcia, Antiscalant cost and maximum water recovery in reverse osmosis for different inorganic composition of groundwater, Desalin. Water Treat. 73 (2017) 46–53.